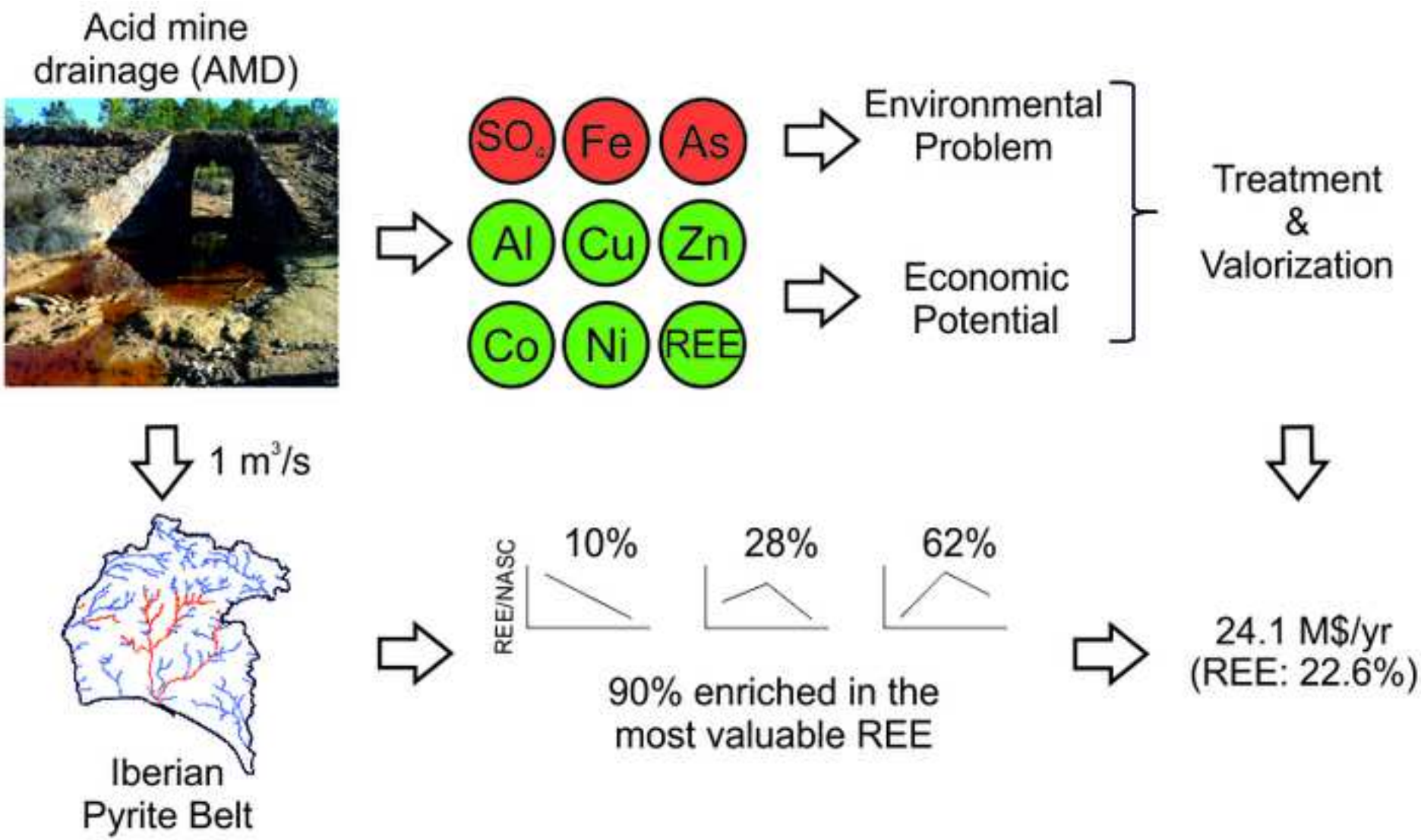

Mine waters as a secondary source of rare earth elements worldwide: the case of the Iberian Pyrite Belt

Rafael León (1*), Francisco Macías (1), Carlos R. Cánovas (1), Rafael Pérez-López (1), Carlos Ayora (2), José Miguel Nieto (1), Manuel Olías (1).

(1) Department of Earth Sciences and Research Center on Natural Resources, Health and the Environment. University of Huelva, Campus "El Carmen", E-21071, Huelva, Spain.

(2) Institute of Environmental Assessment and Water Research, CSIC, Jordi Girona 18, 08034 Barcelona, Spain.

*correspondingauthor: rafael.leon@dct.uhu.es

Abstract

Acid Mine Drainage (AMD) generates a great concern worldwide due to its severe affection to water resources during hundreds and even thousands of years after the cessation of mining activity if control measures are not implemented. AMD treatment is an environmental necessity, but also constitute a tremendous opportunity for the valorization of potential secondary sources of elements of economic interest. The knowledge of the hydrogeochemistry of REE in AMDs and their distribution using normalized patterns would help discrimination of the most potentially marketable AMD sources. To achieve this goal and to estimate the total economic potential of a severely AMD-affected region, chemistry and flow data were determined in spatially and temporally-distributed samples of numerous AMD sources collected throughout the Iberian Pyrite Belt (IPB). Due to high anual metal loads of elements such as Al (6600 ton), Zn (1600 ton), Cu (600 ton), Co (26 ton), Ni (10 ton), LREE (10.7 ton/yr), MREE (2.1 ton/yr), HREE (1 ton/yr), Y (3.7 ton) or Sc (0.7 ton), AMDs of the IPB would have an economic potential of 24.1 M$/yr (being REE 22.6% of this potential). Although the technical and economic limitations would impose a more realistic value of 4.2-10.3 M$/yr. The magnitude of this economic potential cannot be compared with active mines, however the longevity of the AMD generation processes and the need to achieve an environmental improvement make valorization of these leachates an interesting option to recover metals, which would help to treatment plants costs, improving notably the quality of water bodies in abandoned mining sites.

Keywords: Acid Mine Drainage, Valorization, Treatment waste, Metal Load, Critical Raw Materials.

1. Introduction

Acid mine drainages (AMD) are acid leachates with high concentrations of sulfate and metal(loid)s, generated by exposure of sulfides from operating and closed mining sites to oxygen and water (Nordstrom, 1982; Moses et al., 1987). These highly contaminated leachates have become a great concern worldwide (Akcil and Koldas, 2006) for their severe impact to water resources for prolonged periods of time, due to the longevity of AMD generating processes (Younger, 1997; Macías et al., 2017a). According to Johnson and Hallberg. (2005), AMDs can be either treated by active technology, which requires a continuous expense of energy and chemical reagents for its operation; or by passive, which only requires little maintenance and uses energy sources available in nature (dissolution reactions, gravity, microbial activity or photosynthesis). These passive systems face often some technical problems such as Fe and Al armouring and clogging during the treatment of extremely acid and metal-rich AMDs, leading to the loss of treatment effectiveness (Ayora et al., 2013). In recent years, these drawbacks have been overcome using a new passive treatment system known as Dispersed Alkaline Substrate (DAS), which has demonstrated to reduce effectively extreme metal and acidity loads in highly-polluted AMD (Caraballo et al., 2009, 2011b; Macías et al., 2012a,b).

However, the extremely high concentrations of elements of economic interest found in AMDs could provide a potential secondary source of some critical raw materials. Recently, Ayora et al. (2016), Stewart et al. (2017) and Hedin et al. (2019) reported a preferential retention of elements of economic interest, i.e. rare earth elements (REE) and Y, in the solid wastes generated from AMD treatment. Macías et al. (2017b) and Zhang and Honacker (2018, 2020) took a step forward reporting the suitability of recovering these elements (REE and Y) and some other base metals (i.e. Cu, Zn, Co, Ni or Mn) from AMD treatment sludge using dilute commercial acids. The technical feasibility of metal recovery from AMD may convert an environmental problem into a

promising secondary source of raw materials especially for those countries with absence of primary deposits but with a growing demand for base, industrial and technological metals, allowing them not to depend on the supply of other countries (Silberglitt et al., 2013). In addition, this valorization would contribute to face one of the main challenges of mining industry, which is the recycling or reuse of mining wastes, helping to reach a sustainable exploitation of sulfide deposits worldwide (Lottermoser, 2011).

Among the most interesting metals in terms of their potential valorization are REE, a group of 14 elements which often includes two geochemically related elements, such as Sc and Y, and one element that does not have stable isotopes in nature (Pm) (Chakhmouradian et al., 2012). These elements have acquired an ascending importance in recent years, mainly due to their use in diversity of technological applications such as: components of permanent magnets in electric cars and wind turbines, catalysts in the oil refinery and combustion engines, in batteries and other components of electronic devices, in fluorescent tubes for led lighting, or in the fields of nuclear, military, aerospace, and medical technology (Hatch, 2012; Lucas et al., 2014). In 2018, the global rare earth oxides (REOs) production exceeded 190.000 t, of which China produced more than 60% (USGS, 2020).

While natural waters have low REE concentrations, below tens of µg/L (Noack et al., 2014), values exceeding several orders of magnitude can be found in AMD, i.e. between hundreds to thousands of µg/L (Ayora et al., 2016). The longevity of AMD processes, expected to last for hundreds of years, makes AMD a modest but suitable and almost renewable REE source. However, the profitability of the recovery of REE not only depends on the amount contained in AMD and the cost of extraction and separation of a salable concentrate, but also on the proportion of the each REE found in AMD. In this sense, huge differences of price can be found among them in the market, e.g. around 4 $/kg for Ce and around 3120 $/kg for Sc (SMM, 2020).

Therefore, case by case studies worldwide are needed to assess the suitability of AMD as source of raw materials. Because interest in these elements is recent, there are not too many studies globally focused on the potential valorization of REE from AMDs. Although, in recent years, several studies focused on the recovery of REE from AMD sludge in Apalachians coaldfields have been developed (Ziemkiewicz et al., 2016; Stewart et al., 2017; Zhang and Honacker, 2018; 2020; Vass et al., 2019; Hedin et al., 2020).

Regarding this topic, this work is focused on the AMDs of the Iberian Pyrite Belt (IPB), a large metallogenic polymetallic sulfide province located in SW of the Iberian Peninsula, where intensive mining activity has historically been performed (Sanchez-España et al., 2005; Nieto et al., 2013). A preliminary estimation based on average flows of 1 m^3/s of AMD during baseflow conditions and average REE concentration in selected AMD sources, provided an average load of 80 t/yr of REE from the IPB (Ayora et al., 2016). Nevertheless these figures must be more accurately quantified based on larger datasets, including an identification of sources based not only on the total but individual content of REEs due to the economic mismatch in the market between elements of the group.

Therefore, the main objective of this work is the hydrogeochemical characterization of the main AMD sources of the IPB, with special focus on the AMD flow rates, REE concentrations, their normalized distribution pattern and their behavior with respect to the rest of the elements. From this knowledge, the discrimination of the most interesting AMD sources and the estimation of the economic potential of the elements contained in the AMD of this area could be made. This value can be compared with the costs of recovering these metals, wich would suppose a first step in the valorization of these waste streams not only in the IPB, but could also be extended to other mining areas where high flows of AMD with metals of economic interest are generated. However, the economic interest would be even more significant if the calculations

117 consider the AMD contained in other non-renewable sources such as landlocked and
118 pit lakes/ponds, this work only focuses on the draining streams since they suppose
119 almost-renewable resources.

120

121 2. Materials and methods

122 After a preliminary identification of the different AMD sources along the IPB, (Sarmiento
123 et al., 2009), an extensive sampling was performed between 2013 and 2017. A total of
124 126 different AMD sources from 29 mining districts and 5 sub-districts were cataloged
125 and sampled during the study period (Fig. 1, Table S1). In addition, in order to study
126 the seasonal variations of AMD sources, long temporal datasets of selected AMD
127 sources were used: Perrunal mine (06/2010-05/2017, n=55), Esperanza mine
128 (12/2014-02/2018, n=48), Poderosa mine (04/2013-07/2017, n=77) and San Platón
129 mine (02/2015-04/2017, n=33). A total of 339 AMD samples were obtained and used in
130 this study. Immediately after collection, samples were filtered through 0.1 μm Milipore
131 filters, acidulated to pH<2 with HNO_3 suprapur (2 %) and refrigerated until analysis.
132 Different physico-chemical parameters such as pH, oxidation-reduction potential
133 (ORP), electrical conductivity (EC) and temperature were determined in the field using
134 a portable equipment Crison MM40+, previously calibrated with standard solutions for
135 pH (4.01 and 7.00 at 25ºC); EC (147 μS/cm, 1413 μS/cm and 12.88 mS/cm at 25 °C);
136 and checked by the ORP (220 mV and 470 mV at 25ºC). The ORP measurements
137 obtained using the Pt-Ag/AgCl electrode system were corrected for temperature and
138 adjusted to the hydrogen electrode to obtain Eh values (Nordstrom and Wilde, 1998).
139 The analysis of the concentration of major dissolved elements, such as Al, Cu, Fe, Mg,
140 Mn, S and Zn, was performed by Inductively Coupled Plasma-Atomic Emission
141 Spectroscopy (ICP-AES) at the Central Research Services of the University of Huelva.
142 On the other hand, trace elements, such as As, Bi, Cd, Co, Cr, Ga, Ge, Mo, Nb, Ni, Pb,

Sb, Se, Sn, Ta, V, Zr and REE, were analyzed by Inductively Coupled Plasma-Mass Spectroscopy (ICP-MS) in the same laboratory. The detection limits for major elements were: 0.2 mg/L for Al, Cu, Mg, and Zn, 0.1 mg/L for Fe and Mn, and 0.5 mg/L for S, while it was 2 µg/L for trace elements. Triplicate analyses were performed in order to assess the analytical precision, which was below 5% in all samples. In each analysis sequence, blanks were also analyzed, being elements below the detection limits in each blank. The analytical accuracy was confirmed by the analysis of reference materials (NIST-1640).

Flow measurements in each AMD source were made using either a current meter (Global Water FP111) or an electromagnetic current meter (OTT MF pro), while flow data in selected AMD sources to study the seasonal variations were obtained by installing a Parshall flume equipped with a Van Essen level data logger with pressure compensation.

The net acidity (NA) in the samples was estimated using the following equation (Kirby and Cravotta, 2005a,b):

$$NA\ (as\ mg/L\ of\ CaCO_3) = 50045\ (3C_{Al} + 2C_{Fe} + 2C_{Mn} + 2C_{Zn} + 10^{-pH}) - alk$$

Being C_x the molar concentration of Al, Fe, Mn and Zn (mmol/L) and alk the gross alkalinity (mg/L as $CaCO_3$ equivalent).

Rare earth elements were divided into three different sub-groups: light (LREE; from La to Sm), middle (MREE; from Eu to Dy), and heavy (HREE, from Ho to Lu). Different normalization values are available for REEs, e.g. North American Shale Composite (NASC; Taylor and McLennan, 1985), Post-Archean Australian Shale (PAAS; Pourmand et al., 2012) or European Shale (Bau et al., 2018). However, for the study of earth surface processes, such as weathering, REE concentrations are often normalized using the NASC values (Gromet et al., 1984). The normalized REE patterns were

assessed using the NASC-normalized ratios: $(MREE/LREE)_{NASC}$ and $(HREE/MREE)_{NASC}$, calculated as the average of all permutations of those inter-element ratios (Stolpe et al., 2013).

Metal load in each AMD source was estimated based on the concentration of the different metals and the flow measurement. Flow rates are highly variable with season in a Mediterranean climate. Therefore, a coefficient of variation of the metal load was estimated from temporal datasets from Perrunal (n = 55), Esperanza (n = 48), Poderosa (n = 77) and San Platón mine outflows (n=33). This coefficient has been weighted by the number of samples and the coefficient of variation of the metal load of those dataset, as the standard deviation divided by the mean.

To analyze the behavior between the different elements and various parameters, especially with respect to REE, a principal component analysis (PCA) was applied to the chemical data set using the Spearman correlation matrix (Table S4).

3. Results and discussion

3.1 Physico-chemical parameters, major and trace elements of AMD sources

The IPB has a great geological diversity, hosting detrital and chemical sedimentary rocks; acidic, intermediate and basic volcanic, sub-volcanic and volcanic-sedimentary rocks; and massive and disseminate sulfide ores, as main geological units. In addition, these units show a wide range of alteration degrees. A detailed geological description can be found in Saez et al. (1996, 1999) and Tornos (2006). Although the first signs of mining in the IPB date back to pre-Roman times, intensive sulfide exploitation since 1850 was the principal responsible for the currently-abandoned legacy of pit lakes, shafts, galleries, mine wastes or tailing dams (Olías and Nieto, 2015), which favor the sulfide weathering and AMD generation that is then mainly drained by the Tinto and Odiel river basins (Fig. 1). The interaction of the AMD discharges with the different

194 geological units makes possible the existence of a great variety of AMDs in terms of
195 chemical composition.

196 This hydrochemical variety can be observed at pH, which ranges from neutral values
197 (maximum of 6.8) to extremely acid values (minimum of 0.2), being also reflected in net
198 acidity values (Table S2), which can be relatively low (minimum of 18.0 mg/L as
199 $CaCO_3$) or reach maximum of up to 79.6 g/L as $CaCO_3$. The rest of physico-chemical
200 parameters also showed a high variability (Table S2), with EC values ranging from 0.5
201 to 95.8 mS/cm, while the Eh values presented a wide range of positive values (267-815
202 mV), which reflect oxidizing conditions. The temperature also showed some variability
203 depending on the date of sampling, however water temperature is slightly affected by
204 thermalism (interquartile range of 16-23 ºC) associated with the exothermic reaction of
205 sulfide oxidation. Finally, flow ranges from 0.01 to 50 l/s for the different AMD sources.

206 The high variability observed in the AMDs can be also found in the concentration of
207 dissolved elements (Table S3). Figure 2 shows the concentration of some of the major
208 and trace elements analyzed in a box and whiskers plots. The vertical length of the box
209 represents the interquartile range (between the 25th and 75th percentiles), while the
210 horizontal line of its interior represents the median value. The mean is represented by a
211 square, while the lower and upper extreme lines show the minimum and maximum
212 values. As can be seen, the most abundant components are Fe and sulfate (with mean
213 values of 3.1 and 14 g/L and maximum values of 35 and 79 g/L, respectively). Iron and
214 sulfate are released from the oxidative dissolution of pyrite and other sulfides, which
215 also provide high concentrations of other metals such as Cu or Zn (with averages of 99
216 and 244 mg/L, and maximum values of 0.9 and 2.6 g/L, respectively). On the other
217 hand, the interaction of the AMD with the host rocks also causes the occurrence of high
218 concentrations of some elements such as Mg, Al and Mn (mean of 694, 707 and 79
219 mg/L, and maximum of 8.3, 4.1 and 0.9 g/L, respectively).

Concerning trace elements, the dissolution of sulfides also releases other metal(loid)s commonly found in these minerals as impurities such as As (27 mg/L and 2.0 g/L of mean and maximum, respectively), Sb (2.2 and 91 mg/L of mean and maximum, respectively), Cd (0.7 and 16 mg/L of mean and maximum, respectively) and Pb (0.3 and 7.6 mg/L of mean and maximum, respectively). Other trace elements commonly found in the host rocks are V, Cr, Ga and REE with mean values of 713, 258, 224 and 2248 µg/L, respectively, and maximum values of 32.8, 9.7, 8.9 and 12.9 mg/L, respectively. Other trace elements such as Co (4.5 and 30.9 mg/L of mean and maximum, respectively) or Ni (1.2 and 10.7 mg/L of mean and maximum, respectively) can be incorporated not only into the host rock-forming minerals but also into sulfides. Finally, other trace elements such as Bi (490 µg/L), Sn (285 µg/L), Mo (219 µg/L), Zr (94 µg/L), Se (63 µg/L), Be (27 µg/L), Nb (8.0 µg/L), Ta (4.8 µg/L) and Ge (4.6 µg/L) were found at lower mean concentrations, being in some cases (Bi, Ge, Mo, Nb, Sb, Sn, Ta, Zr) close or below detection limits in more than 50% of samples (Table S3).

As can be seen in the modified Ficklin diagram (Fig. 3) for mine water classification based on metallic content and pH (Ficklin et al., 1992), most of the samples (63 %; Fig. 3) are on the field of high-acid (HA) and extreme-metal (EM) waters.However, as already mentioned, some variability in AMD can be observed both in pH, which oscillates between the ultra acid (UA) (close to 0) and near neutral (NN) (pH around 6-7) fields, and in metal content, which varies from ultra-metal (UM) (up to 40 g/L) to low-metal (LM) waters (minimum values of around 50 mg/L). These values can be compared with some AMD examples worldwide such as those generated in coalfields of India (Sahoo et al., 2012; n=12) and Pennsylvania (Cravotta, 2008; n=112), or in pyrite-bearing quartzite quarries of Poland (Migaszewski et al. 2019; n=14) and a metal sulfide mine of Tennessee (Lee et al., 2002; n= 3). In coal mining areas, sulfide-rich wastes also generate high-extreme metal (HM-EM) AMD though with metallic contents 1-2 orders of magnitude lower than those found in the IPB (Fig. 3). The pH values of

coaldfield waters of India are very similar to most of the AMD of the IPB, varying from acid (A) to high acid (HA) waters (pH between 1.6-4.8), while the AMD of Pennsylvania coalfield exhibited less acidity, varying from acid (A) to near neutral (NN) waters (pH between 3.1-6.4; Fig. 3). Meanwhile, AMDs from other sulfide zones are closer to the IPB values. In Tennessee, acid-high acid (A-HA) (pH between 2.2-31) and high-extreme metal (HM-EM) AMDs are recorded, with slightly lower metallic contents than the average of the AMDs from the IPB. On the other hand, the AMDs of Poland have extreme values of Fe and As in ultra-metal (UM) and high-acid (HA) waters (pH between 1.4-2.2), being similar to the most extreme AMDs of the IPB in terms of metal content (Fig. 3). In addition, AMDs from Poland also present extreme REE values (8-22 mg/L), however the highest REE levels were reported in groundwater from Osamu Utsumi uranium mine in Brazil, with values reaching 29 mg/L (Miekeley et al. 1992).

3.2 REE hydrogeochemistry and normalized patterns

It has been widely reported in AMDs that NASC-normalized REE patterns tend to exhibit a convex curvature indicating a MREE enrichment with respect to HREE and LREE (Verplanck et al., 2001; Da Silva et al., 2009; Pérez-López et al., 2010; Sahoo et al., 2012; Ayora et al., 2016). This pattern is also relatively enriched in LREE wih respect to HREE. This fact is not completely explained, although it could be controlled by the Fe cycle. In this sense, Welch et al. (2009) shows an enrichment of LREE in jarosite and its depletion in pore water in acid sulfate soils. The subsequent transformation of jarosite into goethite, which presents a preferential HREE sorption capacity (Verplanck et al., 2004), would lead to the favored release of LREE over HREE in pore water, and therefore explain that asymmetric REE pattern in AMDs.

In the IPB, the average NASC-normalized REE pattern of the AMD samples (n=100; the remaining 26 samples have concentrations close or below the detection limit) coincides with the typical pattern previously reported in AMD, presenting a slight

convex curvature that is indicative of an enrichment of MREE with respect to LREE and HREE, and a slight negative Eu anomaly (Fig.4).

The different AMD samples show an apparent homogeneity in the NASC-normalized REE patterns according to the Figure 4. However, a great variability can be observed in terms of relative enrichment in LREE, MREE and HREE using a Stolpe diagram, which plot NASC-normalized ratios of HREE/MREE vs MREE/LREE (Fig.5; Stolpe et al., 2013).

As can be seen in Fig. 5, AMD samples can be grouped into different fields according to their NASC-normalized REE distributions. This variability is lower in the $(HREE/MREE)_{NASC}$ ratio than in $(MREE/LREE)_{NASC}$ and $(HREE/LREE)_{NASC}$ ones, being all the AMDs enriched in MREE with respect to HREE. Thus, 10% of samples plot on the “type A” field, characterized by being enriched in LREE but depleted in HREE with respect to MREE (Fig. 5). An example of this type of waters would be the acid streams from Confesionarios mine (Fig. S1). The field of “type B” includes 28% of samples, presenting the typical AMD pattern, with a convex curvature enriched in MREE but asymmetric, with greater enrichment of LREE over HREE. An example of these samples would be the underground outflows from San Platón mine (Fig. S1). Finally, the remaining 62% of the AMD samples plot on “type C” pattern field, which is like the previous one, with enrichment in MREE but with opposite asymmetry (enriched in HREE with respect to LREE). The AMD leachates from the Perrunal mine could be a clear example of this type of samples (Fig. S1). These findings show a greater variability in REE patterns of AMDs than that previously reported in literature (Verplanck et al., 2001; Da Silva et al., 2009; Pérez-López et al., 2010; Sahoo et al., 2012; Ayora et al., 2016).

The different REE concentrations and patterns (i.e. types A, B or C) in the AMD may strongly influence the possibility of valorization of these waters. According to this fact, the most promising resources would be the waters located in the “Type C” field (Fig. 5), which are enriched in the most valuable REE (HREE and MREE). On the other hand, “Type B” leachates could also lead to the profitable use of these mine waters due to a predominant MREE content, while "Type A" AMDs, enriched in the least valuable REEs (LREE with respect to MREE and HREE), would have less possibilities of valorization.

Despite the dispersion of REE patterns observed in the Stolpe diagram (Fig. 5), the AMD samples seem to be grouped depending on their origin, since samples collected in the same mine complex are located close each other. This fact suggests that the factor controlling the normalized REE pattern may be the predominant local lithology and mineralogy with which the AMD interacts in each mining complex. Nevertheless, the samples from the Tharsis mining district constitute an exception to this grouping pattern with a very high dispersion among them, which could be due to the historical disposal of wastes from the ore processing from other IPB mining districts and even wastes of other industrial facilities (Moreno-González et al., 2020).

In order to verify this fact, the behavior between the different elements has been analyzed using the PCA applied to the chemical data (Fig. 6), wich could provide new preliminary information about the possible sources of REE in the AMD of the IPB. The first component (PC1) explains 47% of variance and seems to be related to the solubility of the different elements in the pH range of AMDs, with the immobile elements remaining in the negative field and the mobile elements in acidic conditions in the positive field.

Meanwhile, the second component (PC2) explains 12% of the variance, although its relationship is not clear. This component could group the elements according to their mobility during the precipitation of sulfated phases of Fe and Al. In this sense, the main

elements of these minerals (Fe, Al or S) remain in the positive field, in addition to elements that coprecipitate with them, such as As, Ga, Cr, P, Cu or Si, (Lottermoser, 2007), and EC which decreases significantly when precipitating these elements. Divalent metals (Zn, Cd, Mg, Ca, Be, Co, Ni) remain in the negative field, which are in solution at a higher pH. However, this hypothesis is contradicted by the absorption and coprecipitation of REE observed in basaluminite (Ayora et al., 2016).

Another possibility could be the relationship of PC2 with the lithology that releases the different elements into the AMD, remaining in the positive field those elements that mainly come from the oxidation of sulfides (S, Fe, Cu or As) along with parameters strongly influenced by this reaction, such as NA or EC. Furthermore, these elements are located in the diametrically opposite part of the pH, which is inversely influenced by this reaction. On the other hand, the second group includes elements released during the acid dissolution of the host rock, such as Li, Mn, Mg, Ni, Co or U. In this framework, the REE would remain in the negative field, which could preliminarily indicate that the source of these elements in the AMD are the host rocks of the mining systems (Wallrich et al., 2020). An exception is Sc that remains in the positive field, which could be explained due to its different behavior with respect to the rest of REE at low pH (Lozano et al., 2020a). This would be consistent with the results obtained in the NASC-normalized REE distributions (Fig. 5), which show that geology, along with geochemical, biological and environmental factors, may control the REE distribution and patterns in AMD, although more in-depth studies are required to confirm this.

On the other hand, the covariation between HREE, MREE and LREE in AMD has been analyzed in LREE/MREE, LREE/HREE and HREE/MREE correlation graphs (Fig. S2). It can be seen that while HREE and MREE have a good correlation in a single group, the correlation of LREE with both HREE and MREE shows a lower correlation with samples distributed into two well-differentiated groups (groups S2a and S2b). In group S2a, there are samples with a MREE/LREE and HREE/LREE ratio greater than 0.16

and 0.071, respectively, while group S2b corresponds to those samples with a lower ratio. Finally, 10% of the samples present values close to these ratios and their group is undefined as they do not exactly fit both criteria. These correlations could suggest that there may be at least two different sources that contribute REE to the AMDs of IPB, having both the same distribution of HREE and MREE but one of them releasing more LREE into the AMDs. The source that releases more amount of LREE would generate the AMD group S2a while the source with the lower LREE contribution would generate the S2b group.

Finally, it seems reasonable that, although a spatial NASC-normalized REE pattern can be identified at each mining district, the REE concentrations at a same site could fluctuate along the year in response to hydrological conditions, leading to possible changes in the REE patterns. For this reason, the evolution of REE patterns along the time was evaluated for some selected mine discharges: Perrunal (n=55), Esperanza (n=48), Poderosa (n=77) and San Platón (n=33) mines. Figure 7A shows that changes of almost one order of magnitude in the concentration of REE do not imply changes in the NASC-normalized REE pattern, which remains nearly constant. On the other hand, the plotting of these data in the Stolpe diagram (Fig. 7B) shows a slight dispersion of the samples, being grouped according to their location within the IPB. This fact suggests that the changes in concentration observed related to hydrological variations does not induce changes in REE patterns, so, single measurements may be representative of REE patterns in each mine site. This finding contradicts the results recently reported by Moreno-González et al. (2020), which observed during the winter a slight enrichment in LREE and increase in Eu anomalies of AMD from Tharsis mines. However, as stated before, this mining district inherited a vast legacy of mining and mineral processing, resulting in the leaching of a wide variety of mineralized or non-mineralized waste material and rocks with different REE patterns that could have caused such variations.

3.3 Economic potential of AMDs in the IPB. Technical and economic limitations

As stated before, AMDs have high concentrations in elements of high economic potential, and therefore their valorization is an interesting goal. According to the calculations of metal load performed based on flow and concentration data, significant amounts of Al (6600 ton/yr), Cu (600 ton/yr), Zn (1600 ton/yr), Co (25 ton/yr), Ni (10 ton/yr), LREE (10.7 ton/yr), MREE (2.1 ton/yr), HREE (1 ton/yr), Y (3.8 ton/yr), and Sc (0.7 ton/yr) among others, are delivered by AMD sources from the IPB (Table 1). Based on the market prices of these metals (ISE, 2020; LME, 2020; SMM, 2020; USGS, 2020), an estimation of the potential value of the metals released can be performed in around 24.1 M$ per year (Table 1).

Due to its high metal load, the element with the greatest economic potential would be Al (10.5M$/yr) (Table 1), which accounts for 43.6% of the total economic potential. In this sense, the recovery and valorization of Al from AMDs have been previously studied by other authors (Wei et al., 2005; Le et al., 2020). In addition, the profitability of recovering this metal is encouraged by the co-precipitation of Al together with other elements of interest such as Cu or REE in basaluminite (Ayora et al., 2016; Lozano et al., 2020b). In addition, due to their high concentrations in AMDs, the recovery of base metals could be also profitable: 3.8 M$/yr of Cu and 3.3 M$/yr of Zn. On the other hand, it is noticeable that despite being found in lower concentrations, REE represent approximately 22.6% of the total potential valuation of raw materials contained in AMDs of the IPB, with a whole potential value of 5.4 M$/yr. This potential value is not homogeneous, since HREE and Sc represent 10.1% (2.4 M$/yr) and 9.0% (2.2 M$/yr), respectively; whereas MREE, LREE and Y only suppose 2.1, 1.0 and 0.5%, respectively (0.5, 0.25 and 0.12 M$/yr). This supports the significance of HREE and the type of normalized REE pattern for the valorization of AMD, and not the total REE

406 content. In fact, those AMDs enriched in MREE and HREE (‘‘Type C’’ pattern) have an
407 average REE economic potential of 35400 $/yr, twice that of the ‘‘Type B’’ AMDs
408 (18600 $/yr), and an order of magnitude higher than ‘‘type A’’ AMDs (3900 $/yr).
409 However, it should be mentioned that some of these elements, such as Sc and Tm,
410 have a high volatility in prices (Vass et al., 2019) and therefore their final economic
411 potential of said elements is susceptible to variations that must be considered. On the
412 other hand, the recovery of other metals from the AMD, e.g. some technology metals,
413 could be also very interesting economically according to their potential valuation; 0.8
414 M$/yr of Co, 0.14 M$/yr of Be, 0.13 M$/yr of Ni and 0.03 M$/yr of Ga. Finally, there are
415 other elements that, despite their high market value, are found in very low
416 concentrations in AMDs from the IPB and therefore, their recovery seems to be not
417 suitable from both technical and economic points of view (Bi, Cd, Cr, Ge, Mo, Pb, Sb,
418 Sn, Ta or Zr).

419 However, the values above commented are based on single sample metal loads.
420 These amounts are subject to variability due to changes in concentrations and flow
421 rates along the year. In order to consider such variations, the variability associated with
422 temporal datasets from Perrunal (n = 55), Esperanza (n = 48), Poderosa (n = 77) and
423 San Platón (n=33) mine outflows was analyzed and used to estimate maximum and
424 minimum economic potential values (Table 1). The greatest variabilities were found in
425 elements such as Pb, Cu, Se, Ga, Ge, Ni, Cd and Sb (between 45-60% of variation),
426 while elements such as REE, Mo, Co, Cr, Be, Zn and Al, presented a lower variability
427 (35-45%). Finally, the absence (or low representativeness) of data for Bi, Nb, Sn, Ta
428 and Zr hindered the calculation of their variability in AMD sources and, therefore, the
429 average variability (43%) of the rest of elements studied was used. The economic
430 potential value resulting from the application of this variability of the metal load is
431 shown in Table 1.

It has been shown that most of these elements are retained during the treatment of AMD forming a metal-rich sludge (Macías et al., 2017b; Chen et al., 2014), although there are some with low economic potential whose retention is not yet proven (Nb, Ta, Sn or Zr). Nevertheless, data in Table 1 only show the potential value of these elements, though it is not the real value on the market. This assumption is based on the inability to recover all elements contained in AMD, and the existence of impurities in these secondary raw materials. Based on these limitations, a more realistic value could be obtained by applying a reduction percentage of the potential economic value for these metals. In this sense, Smith et al. (2013) reduced by 70% such value based on real cases of valorization of Cu, Zn and Mg in the wastes generated at AMD treatment plants of Berkeley Pit (Montana) and Wellington-Oro (Colorado). After applying this reduction, the potential economic value of raw materials contained in the AMDs from the IPB would range from a minimum of 4.2 M$/yr to a maximum of 10.3 M$/yr.

To avoid these losses in value resulting from the sale of metallic sludge with many impurities, the possibility of processing it in order to achieve their purification should be analyzed. In this sense, to recover these metals from AMD, they must be selectively extracted. As previously reported by Ayora et al. (2016), this separation could be primarily done in the DAS passive treatment plants. These authors reported a sequential separation of metals in several preferential precipitation fronts, where REE along with other metals (mainly Al and Cu) are retained with rates of 0.3% and 1.44% of REE, respectively. Thus, a primary selection of metals to be recovered is performed in the DAS tanks. Then, metals should be subsequently extracted from the sludge. As recently reported by Macías et al. (2017b) and Zhang and Honacker (2018, 2020), it would be easily possible to extract these metals from the sludge only by leaching with diluted acids. The use of 0.5M H_2SO_4 with a solid-liquid ratio of 1:20 was effective for the release of Zn, Cu, Co, Ni and Cd (>90%), and for the leaching of REE (80-90% except for Ce) (Macías et al., 2017b). This generates a leachate with a high amount of

459 different metals (including impurities). Recent studies on selective metal extraction from
460 different aqueous matrices indicate that the recovery of metals from these leachates
461 could be feasible. For example, Cui and Zang (2008) reviewed different approaches
462 based on pyrometalurgical, biometalurgical and hydrometallurgical techniques to
463 recover metals from electronic wastes, while Xie et al. (2014) reviewed the available
464 techniques for the extraction of REE from aqueous solutions. From an economic point
465 of view, the cost of such leaching should be compared to the potential valuation of
466 resources contained in the sludge.

467 There are two full-scale examples of DAS passive treatment plants of AMD in the IPB,
468 where metal-rich sludge is generated (Martínez et al., 2019). The Mina Esperanza DAS
469 passive treatment plant generated around 480 m^3 of metal-rich sludge in its reactive
470 tank after treating 1 L/s of AMD for 840 days (Caraballo et al., 2011a, Orden et al.,
471 2020). On the other hand, the total volume of AMD generated annually in the IPB has
472 been estimated from the flow measurements dataset (n=109) in the AMD sources.
473 Extrapolating the sludge generation at Mina Esperanza to the total AMD of the IPB,
474 around 110000 m^3 of solid wastes would be generated per year after treating 230 L/s of
475 AMD. However, the recovery of metals from some of these wastes would not be
476 profitable due to costs associated with the treatment of AMD, the leaching of metals or
477 the subsequent metallurgical process. It has been considered a unit cost of 0.3 $/$m^3$ for
478 the expenses of construction, maintenance and operation of AMD treatment plants,
479 and unit costs of 100 $/$m^3$ and 1.05 $/$m^3$ for H_2SO_4 and H_2O, respectively necessary
480 for the leaching of metals (Canovas et al., 2019). According to these costs and taking
481 into account only those wastes whose profitability potential exceeds 0.05 M$/yr (at
482 lower profitability unaccounted expenses would be difficult to amortize), around 20
483 sources of a total of 109 could be cost-effectively valorized. These AMDs would
484 generate 47300 m^3 of sludge per year, with a large amount of raw materials contained.
485 Comparing these costs associated with sludge generation and acid leaching (4.5 M$)

with the total valuation, around 24.1 M$/yr, it can be clearly seen that the recovery scheme is profitable. However, some costs such as those asociated with the expenses of metallurgy process to make the selective extraction of the metals and the logistical expenses to put the metals on the market should be included, and therefore the profitability would be significantly reduced.

Raw materials obtained from mining wastes may be currently less profitable than traditional metal production in active mines. However, the recovery of metals from AMD is a promising source of raw materials due fundamentally to two factors: firstly, the longevity of AMD processes, which makes AMD a quasi-renewable poolof metals of economic interest, and lastly, the need to fulfil environmental regulations. The main goal of decision makers in water management at a catchment scale is to mitigate the AMD contamination. These remediation measures are very costly and commonly unaffordable in abandoned mining sites. Thus, the recovery of metals during the AMD treatment would contribute to offset the costs of construction and operation of treatment plants, enhancing the ecological and environmental improvement of the streams affected by these leachates.

4. Conclusions

This study investigates the content in elements of possible economic interest of AMD waters in the IPB, where five active mines and more than one hundred abandoned mining sites are found after intense mining activities. The AMDs of the IPB exhibit a high variability in terms of metal load and physicochemical parameters. Most AMD sources (63%) generate high-acid and extreme-metal waters, being similar to the AMDs generated in other sulfide mining areas, and exceeding even 1-2 orders of magnitude the metal loads reported in coal mining areas worldwide. This is a serious environmental problem, since these AMD sources discharge a high amount of

pollutants to the surrounding water bodies, especially SO_4 or Fe (100000 and 13000 ton/yr respectively).

In these abandoned mining sites, the best option to mitigate pollution is the use of passive treatment methods due to its low cost and need for maintenance. The economic feasibility of applying this technology at a catchment scale could be increased by the valorization of the resulting solid wastes, which contain high amounts of elements with economic potential, thus, helping to offset of the construction costs of the treatment plants. Around 6600 ton of Al, 1600 ton of Zn, 600 ton of Cu, 26 ton of Co, 10 ton of Ni and lower quantities of LREE (10.7 ton), MREE (2.1 ton), HREE (1 ton), Y (3.8 ton), and Sc (0.7 ton) are annually released to the environment from IPB mine sites.

The enrichment in MREE and, above all, HREE of AMDs is a critical factor to be considered in a potential valorization scheme. The NASC-normalized REE patterns from the IPB show a slight convex curvature, indicative of an enrichment of MREE with respect to LREE and HREE and a slight negative Eu anomaly. However, different patterns were observed: 10% of samples have a pattern enriched in LREE and depleted in HREE with respect to MREE, while 62% have convex curvature enriched in MREE with greater enrichment of HREE over LREE. Therefore, 90% of the samples are enriched in the REEs that have the highest economic potential.

On the other hand, multivariate statistical analysis seems to suggest a trend of the elements based on the solubility under acidic conditions. However, a trend can also be observed in the second component whose relationship is more diffuse and that could indicate its dependence on geological control over the release of the different elements into the AMD. According to this hypothesis, the source of REE in the AMD could be related to the acidity leaching of host rock minerals, which would be consistent with the grouping of the samples by mining districts in the Stolpe diagram. Additionally, the

grouping of samples in LREE/MREE and LREE/HREE plots suggests that at least two sources with different LREE release rates could contribute to the REE content in the AMDs.

In terms of economic potential, elements of interest contained in AMD that may be retained in the treatment sludge, would have a total valuation of 24.1 M$/yr, of which Al and REE would account for 43.6 and 22.6% of total respectively, although technical and economic limitations would impose a more realistic value comprised between 4.2-10.3 M$/yr. To avoid these losses, the cost of a pre-treatment focused on purifying the sludge through acid digestion has been analyzed, which would increase the profit margin. A rough estimation on the total costs associated to the treatment of AMD and to recover these metals from the sludge would be 4.5M$/yr. Although to these costs should be added others resulting from metallurgy process or logistical expenses, there is a wide margin with respect to the total valuation of resources. Thus, the recovery of metals during the AMD treatment in abandoned sites worldwide would help to offset the construction and operation costs of treatment plants, improving the quality of the receiving water bodies.

Acknowledgements

This work was supported by the Spanish Ministry of Economy and Competitiveness through the research projects SCYRE (CGL2016-78783-C2-1-R), RENOVAME (FEDER, UHU-1255729) and CAPOTE (CGL2017-86050-R); and the MORECOVERY project of the European Institute of Technology Raw Materials programme. We would also like to thank Dr. Stefano Albanese (Editor-in-Chief), Dr. Annika Parviainen (Guest Editor) and two anonymous reviewers for the support and suggestions that significantly improved the quality of the original paper.

References

Akcil, A., and Koldas, S. (2006). Acid Mine Drainage (AMD): causes, treatment and case studies. Journal of Cleaner Production, 14(12-13), 1139-1145. https://doi.org/10.1016/j.jclepro.2004.09.006

Ayora C., Caraballo M.A., Macías F., Rötting T.S., Carrera J., Nieto J.M. (2013) Acid mine drainage in the Iberian Pyrite Belt: 2. Lessons learned from recent passive remediation experiences. Environmental Science and Pollution Research, 20, 7837–7853. doi:10.1007/s11356-013-1479-2

Ayora C., Macías F., Torres E., Lozano A., Carrero S., Nieto J.M., Pérez-López R., Fernández- Martínez A., and Castillo-Michel H. (2016). Recovery of Rare Earth Elements and Yttrium from Passive-Remediation Systems of Acid Mine Drainage. Environmental Science and Technology, 50, 8255-8262. https://doi.org/10.1021/acs.est.6b02084

Bau, M., Schmidt, K., Pack, A., Bendel, V., & Kraemer, D. (2018). The European Shale: An improved data set for normalisation of rare earth element and yttrium concentrations in environmental and biological samples from Europe. Applied Geochemistry, 90, 142-149. https://doi.org/10.1016/j.apgeochem.2018.01.008

Cánovas, C. R., Chapron, S., Arrachart, G., and Pellet-Rostaing, S. (2019). Leaching of rare earth elements (REEs) and impurities from phosphogypsum: A preliminary insight for further recovery of critical raw materials. Journal of Cleaner Production, 219, 225-235. https://doi.org/10.1016/j.jclepro.2019.02.104

Caraballo M.A., Rötting T.S., Macías F., Nieto J.M., Ayora C. (2009) Field multi-step calcite and MgO passive system to treat acid mine drainage with high metal concentration. Applied Geochemistry, 24, 2301-2311. doi:10.1007/s11356-013-1479-2

588 Caraballo, M. A., Macías, F., Nieto, J. M., Castillo, J., Quispe, D., & Ayora, C. (2011a).
589 Hydrochemical performance and mineralogical evolution of a dispersed alkaline
590 substrate (DAS) remediating the highly polluted acid mine drainage in the full-scale
591 passive treatment of Mina Esperanza (SW Spain). American Mineralogist, 96(8-9),
592 1270-1277. https://doi.org/10.2138/am.2011.3752

593 Caraballo M.A., Macías F., Rötting T.S., Nieto J.M., Ayora C. (2011b) Long term
594 remediation of highly polluted acid mine drainage: a sustainable approach to restore
595 the environmental quality of the Odiel river basin. Environmental Pollution, 159(12),
596 3613-3619. https://doi.org/10.1016/j. envpol.2011.08.003

597 Chakhmouradian, Anton and Wall, F.. (2012). Rare Earth Elements: Minerals, Mines,
598 Magnets (and More). Elements, 8, 333-340.
599 https://doi.org/10.2113/gselements.8.5.333.

600 Chen, T., Yan, B., Lei, C., and Xiao, X. (2014). Pollution control and metal resource
601 recovery for acid mine drainage. Hydrometallurgy, 147, 112-119.
602 https://doi.org/10.1016/j.hydromet.2014.04.024

603 Cravotta, C. A. (2008). Dissolved metals and associated constituents in abandoned
604 coalmine discharges, Pensylvania, USA. Part I: Constituents quantities and
605 correlations. Applied Geochemistry, 23(2), 166−202.
606 https://doi.org/10.1016/j.apgeochem.2007.10.011

607 Cui, J., Zhang, L., (2008). Metallurgical recovery of metals from electronic waste: a
608 review. Journal of hazardous materials, 158, 228-256. DOI:
609 10.1016/j.jhazmat.2008.02.001

610 Da Silva E., Ferreira E., Bobos I., Matos J.X., Patinha C., Reis A.P., and Fonseca E.C.
611 (2009). Mineralogy and geochemistry of trace metals and REE in massive volcanic
612 sulphide host rocks, stream sediments, stream waters and acid mine drainage from the

613 Lousal mine area (Iberian Pyrite Belt, Portugal). Applied geochemistry, 24, 383-401.
614 https://doi.org/10.1016/j.apgeochem.2008.12.001

615 Ficklin WH, Plumlee GS, Smith KS and McHugh JB (1992). Geochemical classification
616 of mine drainages and natural drainages in mineralized areas. Proceedings of the 7th
617 International Symposium on Water Rock Interaction, pp. 381-384.

618 Gromet, L.P., Dymek, R.F., Haskin, L.A., Korotev, R.L., (1984). The "North American
619 shale composite": its compilation, major and trace element characteristics. Geochimica
620 et Cosmochimica Acta, 48, 2469–2482. https://doi.org/10.1016/0016-7037(84)90298-9

621 Hatch GP. (2012). Dynamics in the global market for rare earths. Elements. 8, 341-346.

622 Hedin, B. C., Capo, R. C., Stewart, B. W., Hedin, R. S., Lopano, C. L., and Stuckman,
623 M. Y. (2019). The evaluation of critical rare earth element (REE) enriched treatment
624 solids from coal mine drainage passive treatment systems. International Journal of
625 Coal Geology, 208, 54-64. https://doi.org/10.1016/j.coal.2019.04.007

626 Hedin, B. C., Hedin, R. S., Capo, R. C., & Stewart, B. W. (2020). Critical metal recovery
627 potential of Appalachian acid mine drainage treatment solids. International Journal of
628 Coal Geology, 231, 103610. https://doi.org/10.1016/j.coal.2020.103610

629 ISE, (2020). Institut für seltene Erden und strategische Metalle. https://institut-seltene-
630 erden.de/ (accessed June 2020).

631 Johnson, D. B. and Hallberg, K. B. (2005). Acid mine drainage remediation options: a
632 review. Science of the total environment, 338(1), 3-14.
633 https://doi.org/10.1016/j.scitotenv.2004.09.002

634 Kirby C.S., and Cravotta C.A. (2005a). Net alkalinity and net acidity 1: theoretical
635 considerations. Applied Geochemistry, 20, 1920-1940.
636 https://doi.org/10.1016/j.apgeochem.2005.07.002

637 Kirby C.S., and Cravotta C.A. (2005b). Net alkalinity and net acidity 2: practical
638 considerations. Applied Geochemistry, 20, 1941-1964.
639 https://doi.org/10.1016/j.apgeochem.2005.07.003

640 Lee, G., Bigham, J.M., Faure, G., (2002). Removal of trace metals by coprecipitation
641 with Fe, Al and Mn from natural waters contaminated with acid mine drainage in the
642 Ducktown Mining District, Tennessee. Applied Geochemistry, 17, 569-581.
643 https://doi.org/10.1016/S0883-2927(01)00125-1.

644 Le, V.G., Vo, T.D.H., Nguyen, B.S., Vu, C.T., Shih, Y.J., Huang, Y.H. (2020). Recovery
645 of iron (II) and aluminum (III) from acid mine drainage by sequential selective
646 precipitation and fluidized bed homogeneous crystallization (FBHC). Journal of the
647 Taiwan Institute of Chemical Engineers, 115, 135-143.
648 https://doi.org/10.1016/j.jtice.2020.10.007

649 LME, (2020). London Metal Exchange Official Prices for Metal Global Market.
650 https://www.lme.com/ (accessed June 2020).

651 Lottermoser, B. G. (2007). Mine wastes: characterization, treatment, environmental
652 impacts. Berlin.

653 Lottermoser, B. G. (2011). Recycling, reuse and rehabilitation of mine wastes.
654 Elements, 7, 405-410. https://doi.org/10.2113/gselements.7.6.405

655 Lozano, A., Ayora, C., & Fernández-Martínez, A. (2020a). Sorption of rare earth
656 elements on schwertmannite and their mobility in acid mine drainage treatments.
657 Applied Geochemistry, 113, 104499. https://doi.org/10.1016/j.apgeochem.2019.104499

658 Lozano, A., Ayora, C., Macías, F., León, R., Gimeno, M. J., & Auqué, L. (2020b).
659 Geochemical behavior of rare earth elements in acid drainages: Modeling
660 achievements and limitations. Journal of Geochemical Exploration, 106577. DOI:
661 10.1016/j.gexplo.2020.106577

662 Lucas, J., Lucas, P., Le Mercier, T., Rollat, A., and Davenport, W. G. (2014). Rare
663 earths: science, technology, production and use. Elsevier.

664 Macías F., Caraballo M.A., Nieto J.M., Rötting T.S., Ayora C. (2012a) Natural
665 pretreatment and passive remediation of highly polluted acid mine drainage. Journal of
666 environmental management, 104, 93–100. doi: 10.1016/j.jenvman.2012.03.027

667 Macías F., Caraballo M.A., Rötting T.S., Pérez-López R., Nieto J.M., Ayora C. (2012b)
668 From highly polluted Zn-rich acid mine drainage to non-metallic waters: implementation
669 of a multi-step alkaline passive treatment system to remediate metal pollution. Science
670 of the total environment, 433, 323–330. doi: 10.1016/j.scitotenv.2012.06.084

671 Macías, F., Pérez-López, R., Caraballo, M.A., Sarmiento, A.M., Cánovas, C.R.,Nieto,
672 J.M., Olías, M., Ayora, C., (2017a). A geochemical approach to the restoration plans for
673 the Odiel River basin (SW Spain), a watershed deeply polluted by acid mine drainage.
674 Environmental Science and Pollution Research, 24, 4506-4516.
675 https://doi.org/10.1007/s11356-016-8169-9.

676 Macías, F., Pérez-López, R., Caraballo, M.A., Cánovas, C.R., Nieto, J.M., (2017b).
677 Management strategies and valorization for waste sludge from active treatment of
678 extremely metal-polluted acid mine drainage: a contribution for sustainable mining.
679 Journal of Cleaner Production, 141, 1057-1066.
680 https://doi:10.1016/j.jclepro.2016.09.181.

681 Martínez, N. M., Basallote, M. D., Meyer, A., Cánovas, C. R., Macías, F., and
682 Schneider, P. (2019). Life cycle assessment of a passive remediation system for acid
683 mine drainage: towards more sustainable mining activity. Journal of Cleaner
684 Production, 211, 1100-1111. https://doi.org/10.1016/j.jclepro.2018.11.224

685 Miekeley, N., de Jesus, H. C., da Silveira, C. P., Linsalata, P., & Morse, R. (1992).
686 Rare-earth elements in groundwaters from the Osamu Utsumi mine and Morro do

687 Ferro analogue study sites, Poços de Caldas, Brazil. Journal of Geochemical
688 Exploration, 45(1-3), 365-387.

689 Migaszewski, Z. M., Gałuszka, A., & Dołęgowska, S. (2019). Extreme enrichment of
690 arsenic and rare earth elements in acid mine drainage: case study of Wiśniówka mining
691 area (south-central Poland). Environmental pollution, 244, 898-906.
692 https://doi.org/10.1016/j.envpol.2018.10.106

693 Moreno-González, R., Cánovas, C. R., Olías, M., and Macías, F. (2020). Seasonal
694 variability of extremely metal rich acid mine drainages from the Tharsis mines (SW
695 Spain). Environmental Pollution, 259, 113829.
696 https://doi.org/10.1016/j.envpol.2019.113829

697 Moses C.O., Nordstrom D.K., Herman J.S., and Mills A.L. (1987). Aqueous pyrite
698 oxidation by disolved oxygen and by ferric iron. Geochimica et Cosmochimica Acta, 51,
699 1561-1571. https://doi.org/10.1016/0016-7037(87)90337-1

700 Nieto, J. M., Sarmiento, A. M., Canovas, C. R., Olias, M., and Ayora, C. (2013). Acid
701 mine drainage in the Iberian Pyrite Belt: 1. Hydrochemical characteristics and pollutant
702 load of the Tinto and Odiel rivers. Environmental Science and Pollution Research,
703 20(11), 7509-7519. DOI: 10.1007/s11356-013-1634-9

704 Noack C.W., Dzombak D.A., and Karamalidis A.K. (2014) Rare Earth Element
705 Distributions and Trends in Natural Waters with a Focus on Groundwater.
706 Environmental Science and Technology, 48, 4317- 4326. DOI: 10.1021/es4053895

707 Nordstrom D.K. (1982). Aqueous pyrite oxidation and the consequent formation of
708 secondary iron minerals. In: Kittrick JA, Fanning DS and Hossner LR (Eds.): Acid
709 Sulfate Weathering. Soil Science Society of America Special Publication 10, pp. 37-56.

710 Nordstrom, D. K., & Wilde, F. D. (1998). Reduction–oxidation potential (electrode
711 method). National Field Manual for the Collection of Water Quality Data, book 9,

712 chapter 6.5. US Geological Survey techniques of water-resources investigations, US
713 Geological Survey, Reston, VA (20 pp.).

714 Olías, M., & Nieto, J. M. (2015). Background conditions and mining pollution throughout
715 history in the Río Tinto (SW Spain). Environments, 2(3), 295-316.
716 https://doi.org/10.3390/environments2030295

717 Orden, S., Macías, F., Cánovas, C. R., Nieto, J. M., Pérez-López, R., & Ayora, C.
718 (2020). Eco-sustainable passive treatment for mine waters: Full-scale and long-term
719 demonstration. Journal of Environmental Management, 111699.
720 https://doi.org/10.1016/j.jenvman.2020.111699

721 Pérez-López R., Delgado J., Nieto J.M., and Márquez-García B. (2010). Rare earth
722 element geochemistry of sulphide weathering in the São Domingos mine area (Iberian
723 Pyrite Belt): A proxy for fluid-rock interaction and ancient mining pollution. Chemical
724 Geology, 276, 29- 40. https://doi.org/10.1016/j.chemgeo.2010.05.018

725 Pourmand, A., Dauphas, N., & Ireland, T. J. (2012). A novel extraction chromatography
726 and MC-ICP-MS technique for rapid analysis of REE, Sc and Y: Revising CI-chondrite
727 and Post-Archean Australian Shale (PAAS) abundances. Chemical Geology, 291, 38-
728 54. https://doi.org/10.1016/j.chemgeo.2011.08.011

729 Sáez, R., Almodóvar, G. R., and Pascual, E. (1996). Geological constraints on massive
730 sulphide genesis in the Iberian Pyrite Belt. Ore Geology Reviews, 11(6), 429-451.

731 Sáez, R., Pascual, E., Toscano, M., and Almodóvar, G. R. (1999). The Iberian type of
732 volcano-sedimentary massive sulphide deposits. Mineralium Deposita, 34(5-6), 549-
733 570. https://doi.org/10.1016/S0169-1368(96)00012-1

734 Sahoo P.K., Tripathy S., Equeeniddin S.M., and Panigrahi M.K. (2012). Geochemical
735 characteristics of coal mine discharge vis-à-vis behaviour of rare earth elements at

736 Jaintia Hills coalfield, northeastern India. Journal of Geochemical Exploration 112, 235-
737 246. https://doi.org/10.1016/j.gexplo.2011.09.001

738 Sánchez-España J., López Pamo E., Santofimia E., Aduvire O., Reyes J., and
739 Barettino D. (2005). Acid mine drainage in the Iberian Pyrite Belt (Odiel river
740 watershed, Huelva, SW Spain): geochemistry, mineralogy and environmental
741 implications. Applied geochemistry, 20(7), 1320-1356.
742 https://doi.org/10.1016/j.apgeochem.2005.01.011

743 Sarmiento, A. M., Nieto, J. M., Olías, M., and Cánovas, C. R. (2009). Hydrochemical
744 characteristics and seasonal influence on the pollution by acid mine drainage in the
745 Odiel river Basin (SW Spain). Applied Geochemistry, 24(4), 697-714.
746 https://doi.org/10.1016/j.apgeochem.2008.12.025

747 Silberglitt, R., Bartis, J.T., Chow, B.G., An, D.L., Brady, K., 2013. Critical Materials:
748 Present Danger to U.S. Manufacturing. RAND Corporation, Santa Monica, CA.
749 www.rand.org/pubs/research_reports/RR133.

750 SMM, (2020). Shangai Metals Market. https://www.metal.com/ (accessed June 2020).

751 Smith K.S., Figueroa L.A., and Plumlee G.S. (2013). Can treatment and disposal costs
752 be reduced through metal recovery? International Mine Water Association Conference
753 IMWA2013 -Reliable Mine Water Technology (Golden, Colorado) 729-734.

754 Stewart, B. W., Capo, R. C., Hedin, B. C., and Hedin, R. S. (2017). Rare earth element
755 resources in coal mine drainage and treatment precipitates in the Appalachian Basin,
756 USA. International Journal of Coal Geology, 169, 28-39.
757 https://doi.org/10.1016/j.coal.2016.11.002

758 Stolpe B., Guo L., and Shiller A.M. (2013). Binding and transport of rare earth elements
759 by organic and iron-rich nanocolloids in Alaskan rivers, as revealed by field-flow

760 fractionation and ICP-MS. Geochimica et Cosmochimica Acta 106, 446-462.
761 https://doi.org/10.1016/j.gca.2012.12.033

762 Taylor, S.R. and McLennan, S.M. (1985) The Continental Crust: Its Composition and
763 Evolution. Blackwell, Oxford, 1-312.

764 Tornos F. (2006). Environment of formation and styles of volcanogenic massive
765 sulfides: the Iberian Pyrite Belt. Ore Geology Reviews, 28, 259-307.
766 https://doi.org/10.1016/j.oregeorev.2004.12.005

767 USGS, 2020. Mineral Commodity Summaries 2020. U.S. Geological Survey, 2020,
768 Mineral Commodity Summaries 2020. U.S. Geological Survey. 204p.
769 https://doi.org/10.3133/mcs2020

770 Vass, C. R., Noble, A., and Ziemkiewicz, P. F. (2019). The Occurrence and
771 Concentration of Rare Earth Elements in Acid Mine Drainage and Treatment By-
772 products: Part 1—Initial Survey of the Northern Appalachian Coal Basin. Mining,
773 Metallurgy and Exploration, 36(5), 903-916. DOI: 10.1007/s42461-019-0097-z

774 Verplanck, P. L., Antweiler, R. C., Nordstrom, D. K., & Taylor, H. E. (2001). Standard
775 reference water samples for rare earth element determinations. Applied Geochemistry,
776 16(2), 231-244. https://doi.org/10.1016/S0883-2927(00)00030-5

777 Verplanck, P. L., Nordstrom, D. K., Taylor, H. E., & Kimball, B. A. (2004). Rare earth
778 element partitioning between hydrous ferric oxides and acid mine water during iron
779 oxidation. Applied Geochemistry, 19(8), 1339-1354.
780 https://doi.org/10.1016/j.apgeochem.2004.01.016

781 Wallrich, I. L., Stewart, B. W., Capo, R. C., Hedin, B. C., & Phan, T. T. (2020).
782 Neodymium isotopes track sources of rare earth elements in acidic mine waters.
783 Geochimica et Cosmochimica Acta, 269, 465-483.
784 https://doi.org/10.1016/j.gca.2019.10.044

785 Wei, X., Viadero Jr, R. C., & Buzby, K. M. (2005). Recovery of iron and aluminum from
786 acid mine drainage by selective precipitation. Environmental Engineering Science,
787 22(6), 745-755. DOI: 10.1089/ees.2005.22.745

788 Welch S.A., Christy A.G., Isaacson L., and Kirste D. (2009). Mineralogical control of
789 rare earth elements in acid sulfate soils. Geochimica et Cosmochimica Acta, 73, 44-64.
790 https://doi.org/10.1016/j.gca.2008.10.017

791 Xie, F., Zhang, T. A., Dreisinger, D., and Doyle, F. (2014). A critical review on solvent
792 extraction of rare earths from aqueous solutions. Minerals Engineering, 56, 10-28.
793 https://doi.org/10.1016/j.mineng.2013.10.021

794 Younger, P.L., 1997. The longevity of minewater pollution: a basis for decision making.
795 Science of the total environment, 194-195, 457-466. https://doi.org/10.1016/S0048-
796 9697(96)05383-1

797 Zhang, W., and Honaker, R. Q. (2018). Rare earth elements recovery using staged
798 precipitation from a leachate generated from coarse coal refuse. International Journal
799 of Coal Geology, 195, 189-199. https://doi.org/10.1016/j.coal.2018.06.008

800 Zhang, W., and Honaker, R. (2020). Process development for the recovery of rare
801 earth elements and critical metals from an acid mine leachate. Minerals Engineering,
802 153, 106382. https://doi.org/10.1016/j.mineng.2020.106382

803 Ziemkiewicz, P., He, T., Noble, A., and Liu, X. (2016). Recovery of rare earth elements
804 (REEs) from coal mine drainage. US Department of Energy, National Energy
805 Technology Laboratory.

806 ## Figure Caption

807 Figure 1. Location map indicating the main water courses draining the IPB and sampling points.
808 A detailed view can be consulted in the KML file (Google Earth™) available as electronic

809 supplement, and a list with UTM geographic location and mining district associated with each
810 sampling point can be seen in Table S1.

811 Figure 2. Box-and-whiskers plot of dissolved concentrations of major A) and trace elements B)
812 in AMD samples collected in this study (n=126). See the text for explanation.

813 Figure 3. Modified Ficklin diagram of collected AMD samples according to their pH values and
814 metal concentrations. Examples of AMDs from coalfields in India (Sahoo et al., 2012) and
815 Pennsylvania (Cravotta, 2008), from sulfide mines in Tennessee (Lee et al., 2002) and pyrite-
816 bearing quartzite quarries in Poland (Migaszewski et al., 2019). UA: ultra acid, HA: high acid,
817 A: acid, NN: near neutral, UM: ultra metal, EM: extreme metal, AM: high metal, LM: low metal.

818 Figure 4. Range (Minimum-Maximum) and average of NASC-normalized REE patterns of AMDs
819 in this study (n = 100).

820 Figure 5. Diagram of AMD samples according to their relative contents of LREE, MREE and
821 HREE (in log scale) normalized to NASC (modified from Stolpe et al., 2013). The different
822 symbols refer to different mining districts of the IPB (Table S1). In each field, a graph indicating
823 the enrichment type is shown. In these insets, C_N refers to the NASC-normalized concentration
824 and Z→ refers to the REE in order by their increasing atomic number.

825 Figure 6. Principal component analysis (PCA) applied to chemical dataset. The Spearman
826 correlation matrix applied to the chemical data set is available as an electronic supplement
827 (Table S4).

828 Figure 7.A: NASC-normalized REE pattern variability in selected AMD sources of the IPB. B:
829 Diagram of temporal datasets of AMDs according to their relative contents of LREE, MREE and
830 HREE normalized to NASC (modified from Stolpe et al., 2013).

831

832 ## Supplementary Information

833 Table S1. UTM geographic location and mining district associated with each sampling
834 point.

KMZ S1. KML file (Google Earth™) with the location of each sampling point.

Table S2. Statistical parameters of AMD samples collected in the IPB (n=126).

Figure S1. Examples of representative NASC-normalized REE patterns observed in AMD samples collected in this study.

Table S3. Statistical parametres of disolved elements of AMD samples in the IPB (n=128).

Table S4. Spearman correlation matrix aplied to chemical dataset.

Figure S2. LREE/MREE, LREE/HREE and HREE/MREE correlation graphs of AMD samples.

Figure1

Click here to access/download;Figure;Figure1.jpg

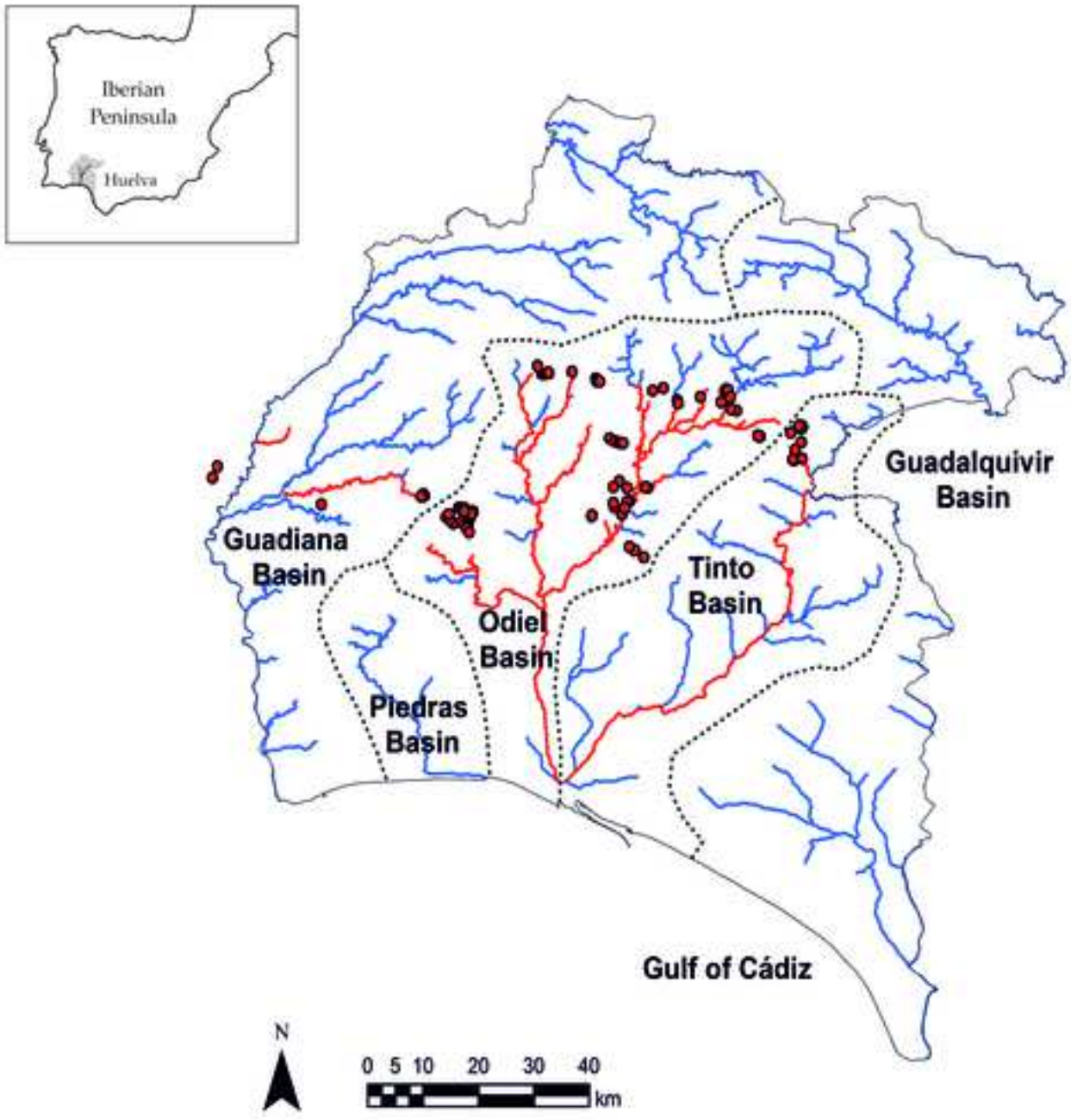

Figure2

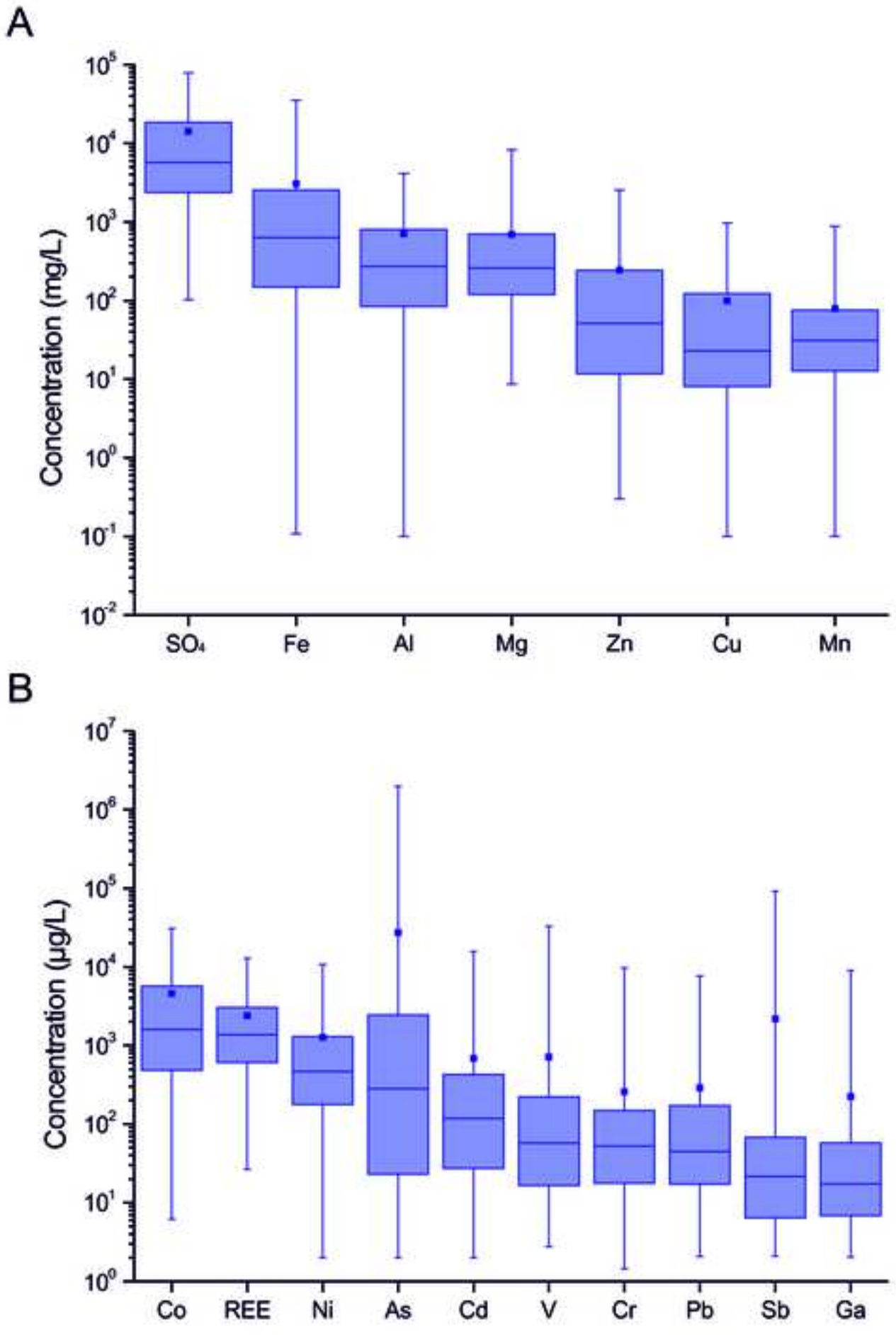

Figure3

Click here to access/download;Figure;Figure3.jpg

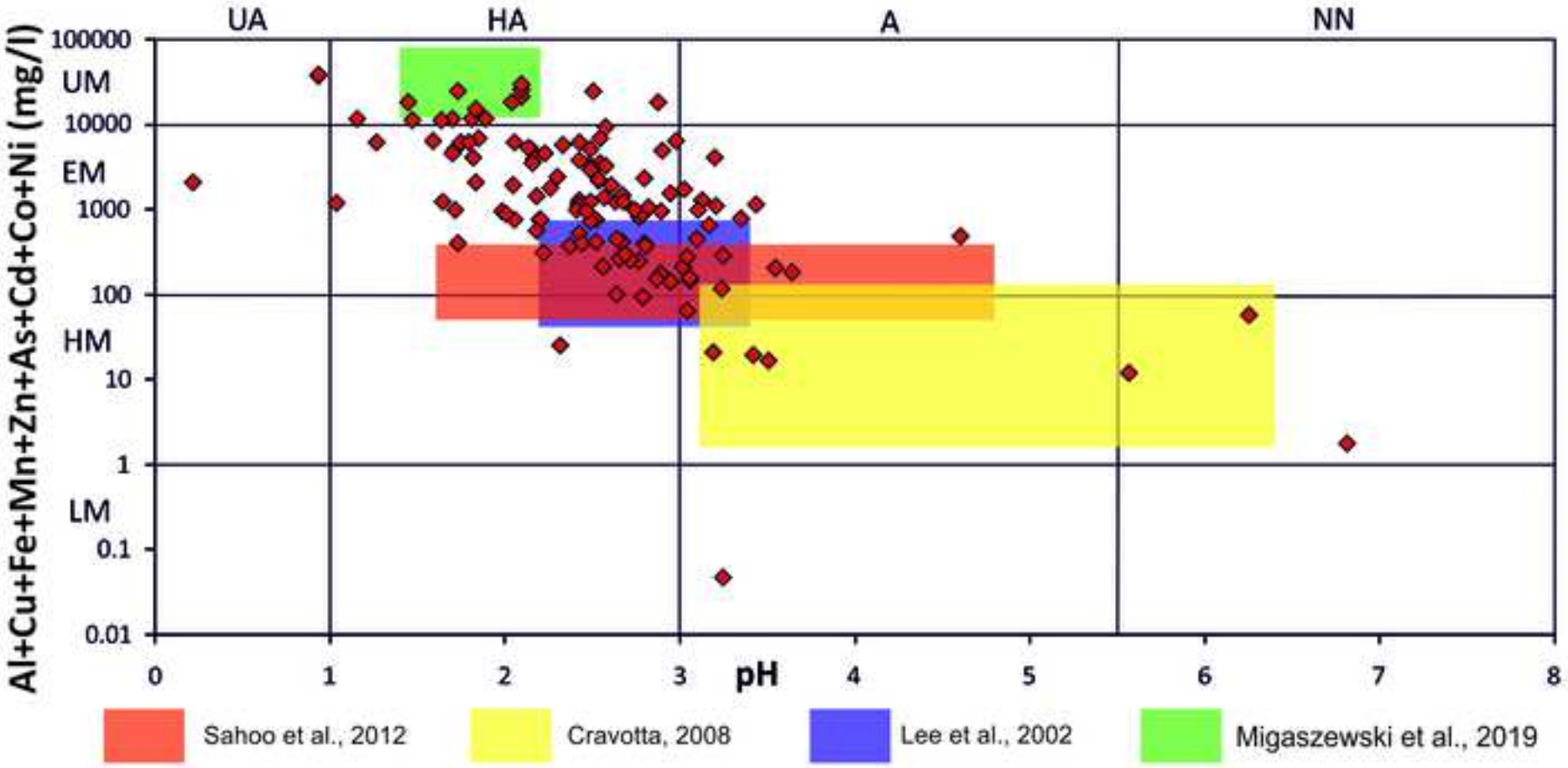

Figure4

Click here to access/download;Figure;Figure4.jpg

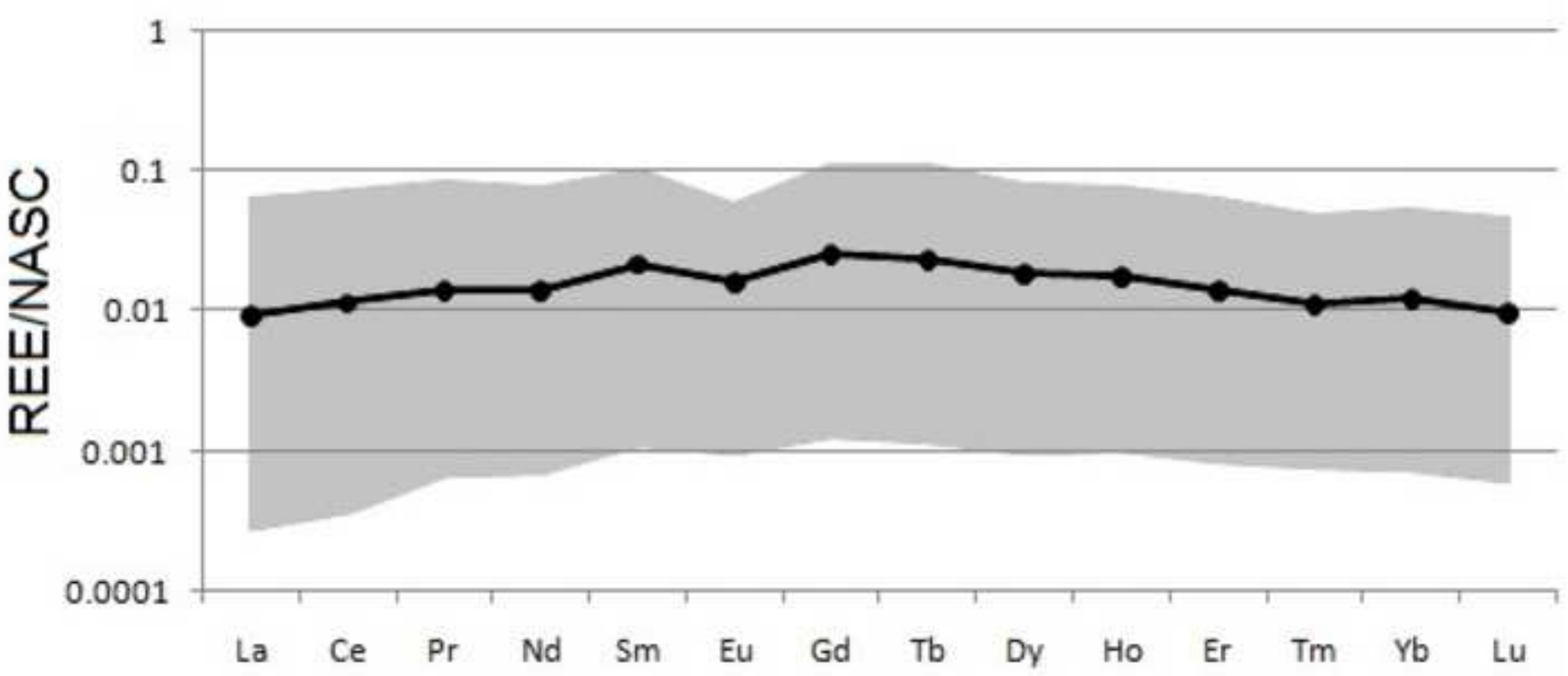

Figure5

Click here to access/download;Figure;Figure5.jpg

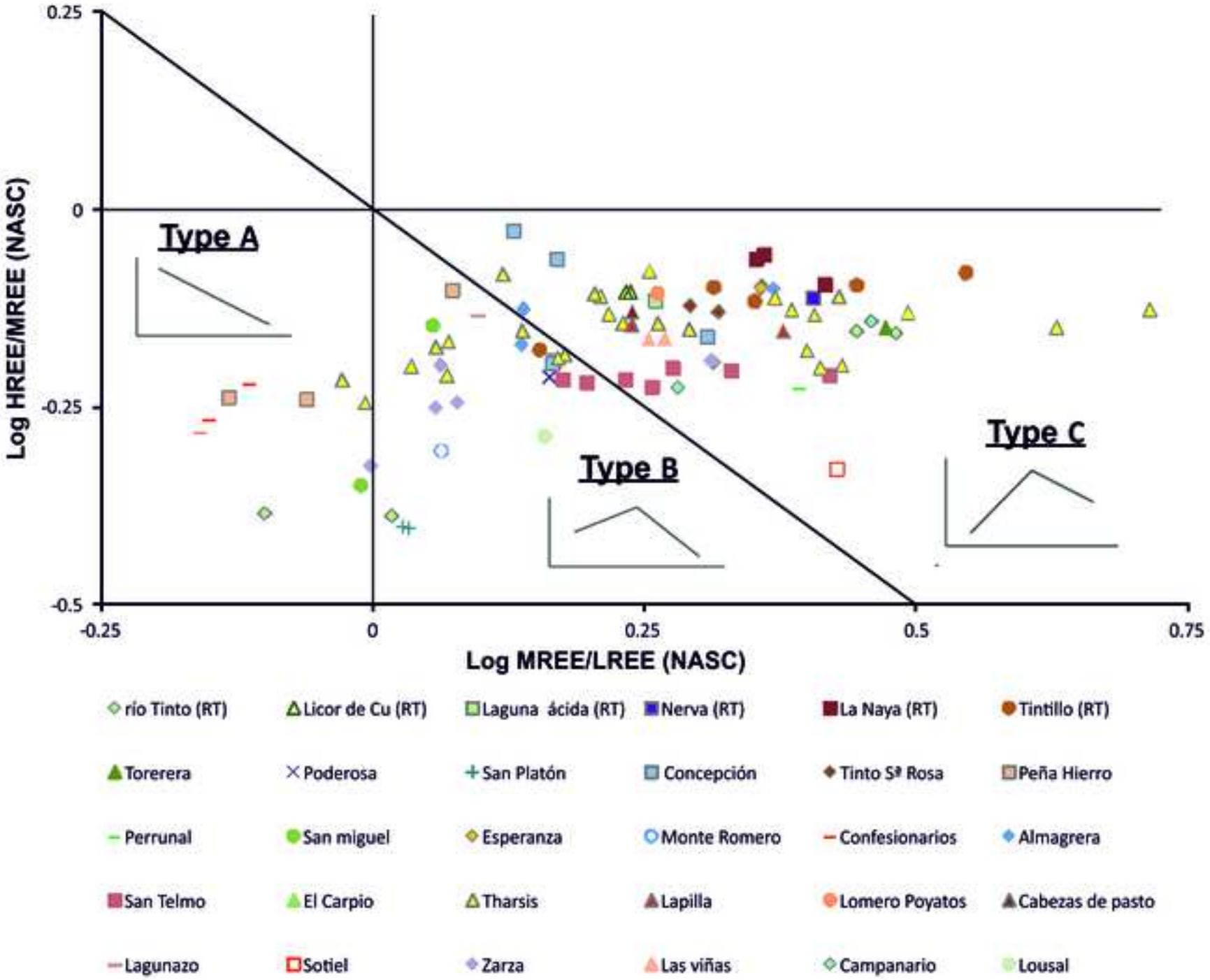

Figure6

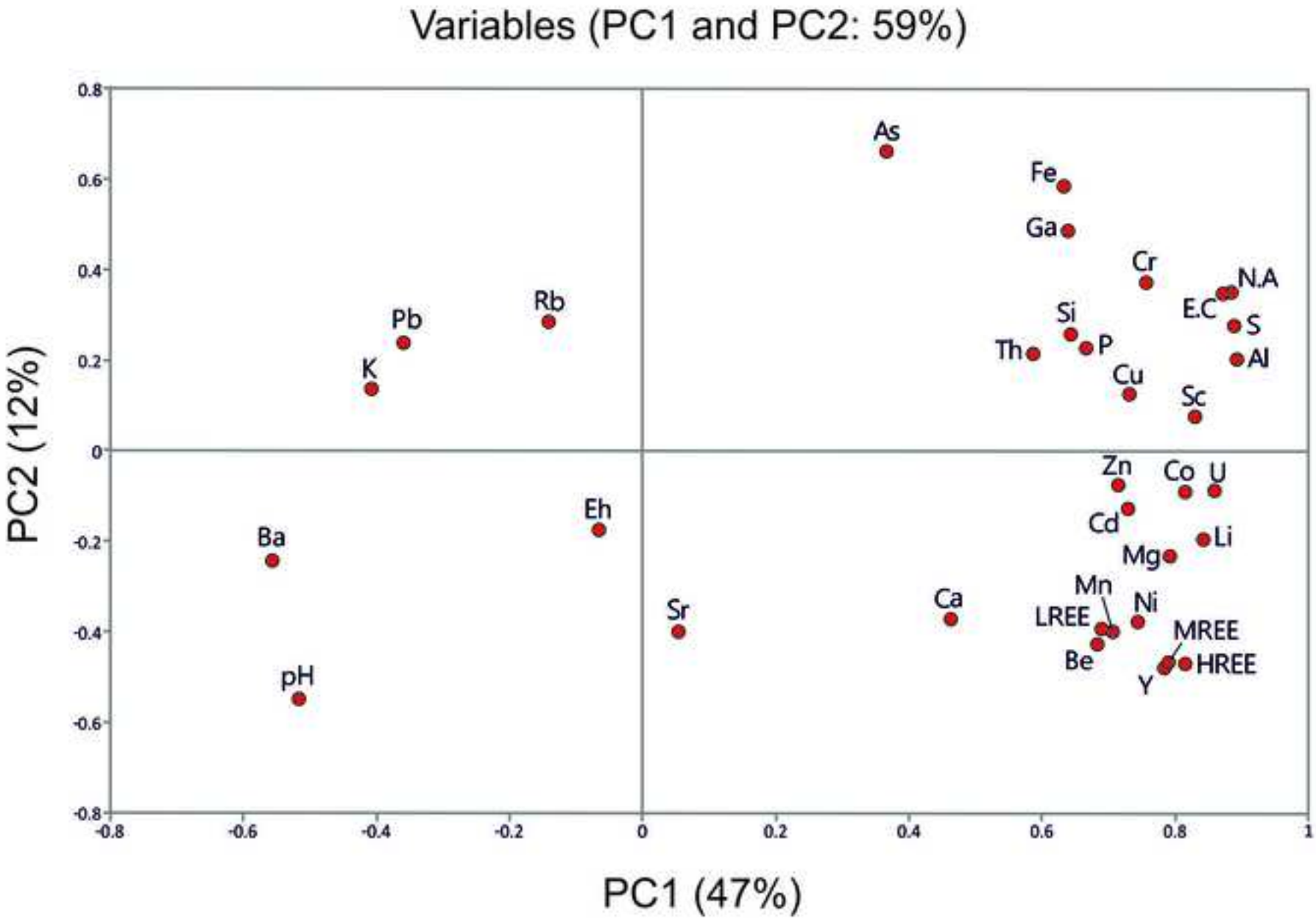

Figure7

Click here to access/download;Figure;Figure7.jpg

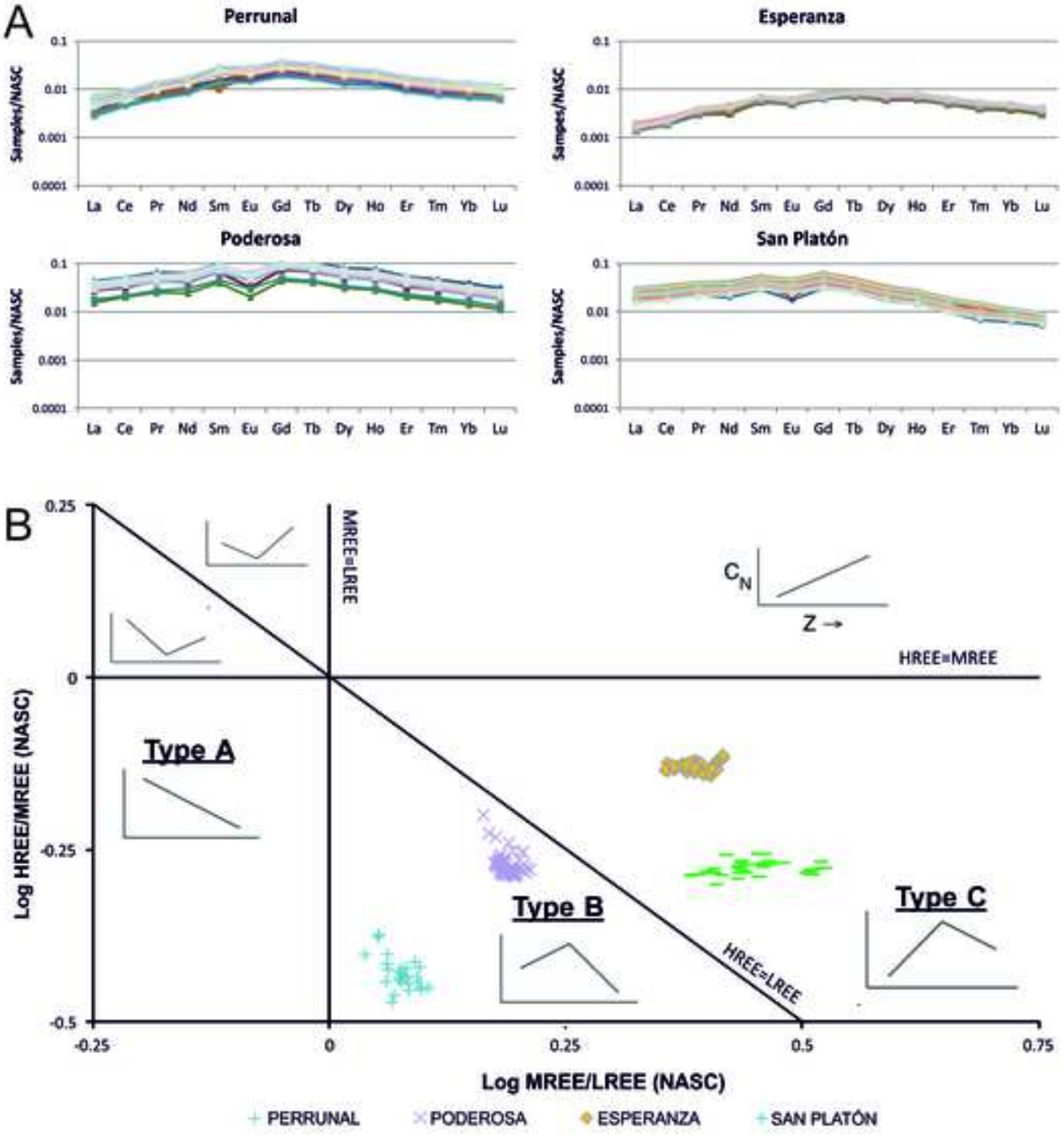

Table 1. Estimated yearly metal pool and potential valuation of the elements of economic interest contained in AMDs of the IPB.

	Metal load	Price	Avrg economic potential		CV metal load	Max economic potential		Min economic potential	
	(ton/yr)	(k$/ton)	(M$/yr)	(k$/yr)	(%)	(M$/yr)	(k$/yr)	(M$/yr)	(k$/yr)
Al	6598.9	1.6	10.5	-	38	14.6	-	6.5	-
Cu	625	6	3.8	-	53	5.8	-	1.8	-
Zn	1618.3	2	3.3	-	40	4.6	-	1.9	-
Tm	0.05	50000	2.4	-	39	3.3	-	1.5	-
Sc	0.69	3120	2.2	-	44	3.1	-	1.2	-
Co	26.38	30	0.8	-	43	1.1	-	0.5	-
Dy	0.85	362	0.3	-	41	0.4	-	0.2	-
Nd	2.79	53.9	0.15	-	41	0.21	-	0.09	-
Be	0.17	863	0.14	-	41	0.2	-	0.09	-
Ni	9.83	12.9	0.13	-	46	0.19	-	0.07	-
Tb	0.15	831	0.13	-	39	0.18	-	0.08	-
Y	3.76	30.9	0.12	-	40	0.16	-	0.07	-
Pr	0.64	90	0.06	-	41	0.08	-	0.03	-
Eu	0.14	285	0.04	-	41	0.05	-	0.02	-
Ga	0.19	145	-	27.4	48	-	40.5	-	14.3
Lu	0.04	618	-	25.9	37	-	35.5	-	16.3
Gd	0.95	25.7	-	24.4	41	-	34.3	-	14.4
Ce	4.83	4	-	19.4	40	-	27.3	-	11.6
Sm	0.83	13.1	-	10.8	42	-	15.4	-	6.3
Er	0.39	22.6	-	8.9	39	-	12.4	-	5.4
Ho	0.15	58.2	-	8.7	39	-	12.1	-	5.3
Cd	3.32	2.6	-	8.5	45	-	12.4	-	4.7
Mo	0.29	26	-	7.5	43	-	10.7	-	4.3
La	1.62	4.5	-	7.2	43	-	10.3	-	4.2
Zr	0.06	100	-	6.3	43	-	8.9	-	3.6
Ge	0.01	1028	-	5.5	47	-	8	-	2.9
Yb	0.33	14.8	-	4.9	39	-	6.8	-	2.9
Cr	0.56	8	-	4.5	43	-	6.4	-	2.6
Se	0.2	18.5	-	3.7	50	-	5.5	-	1.8
Ta	0.01	152	-	2.2	43	-	3.2	-	1.3
Pb	0.71	1.7	-	1.2	60	-	1.9	-	0.5
Sb	0.19	5.7	-	1.1	45	-	1.5	-	0.6
Bi	0.05	19.8	-	1	43	-	1.4	-	0.6
Sn	0.01	16	-	0.09	43	-	0.13	-	0.05
Nb	0.001	29.4	-	0.04	43	-	0.06	-	0.02
Total	-	-	24.1 (M$/yr)		42	34.2 (M$/yr)		14.0 (M$/yr)	

Avrg: Average. CV: Coefficient of variation. Max: Maximun. Min: Minimun.

Figure S1


Click here to access/download
Supplementary Material
Figure_S1.jpg

Figure_S2

Table S1


Click here to access/download
Supplementary Material
Table_S1.xlsx

Table S2


Click here to access/download
Supplementary Material
Table_S2.xlsx

Table S3

Click here to access/download
Supplementary Material
Table_S3.xlsx

Table S4

Click here to access/download

Interactive Map Data (.kml, .kmz)

KMZ_S1.kml